

Effect of the technological conditions of frictional treatment on the structure, phase composition and hardening of metastable austenitic steel

Cite as: AIP Conference Proceedings **1785**, 040035 (2016); <https://doi.org/10.1063/1.4967092>
Published Online: 18 November 2016

A. V. Makarov, P. A. Skorynina, A. S. Yurovskikh, and A. L. Osintseva



View Online



Export Citation

ARTICLES YOU MAY BE INTERESTED IN

[Effect of preliminary nanostructuring frictional treatment on the efficiency of nitriding of metastable austenitic steel in electron beam plasma](#)

AIP Conference Proceedings **1915**, 030011 (2017); <https://doi.org/10.1063/1.5017331>

[Eddy-current testing of fatigue degradation upon contact fatigue loading of gas powder laser clad NiCrBSi-Cr₃C₂ composite coating](#)

AIP Conference Proceedings **1915**, 040049 (2017); <https://doi.org/10.1063/1.5017397>

[Increasing the micromechanical and tribological characteristics of an austenitic steel by surface deformation processing](#)

AIP Conference Proceedings **2053**, 030064 (2018); <https://doi.org/10.1063/1.5084425>



Your Qubits. Measured.

Meet the next generation of quantum analyzers

- Readout for up to 64 qubits
- Operation at up to 8.5 GHz, mixer-calibration-free
- Signal optimization with minimal latency

Find out more

 Zurich Instruments

Effect of the Technological Conditions of Frictional Treatment on the Structure, Phase Composition and Hardening of Metastable Austenitic Steel

A.V. Makarov^{1,2}, P.A. Skorynina^{1, a)}, A.S. Yurovskikh³, A.L. Osintseva¹

¹*Institute of Engineering Science, Ural Branch of the Russian Academy of Sciences, 34 Komsomolskaya st., Ekaterinburg, 620049 Russia*

²*M.N. Miheev Institute of Metal Physics, Ural Branch of the Russian Academy of Sciences, 18 S. Kovalevskoy st., Ekaterinburg, 620990 Russia*

³*Ural Federal University named after the first President of Russia B.N. Yeltsin, 19 Mira st., Ekaterinburg, 620002 Russia*

^{a)}Corresponding author: skorynina@imach.uran.ru

Abstract. The process parameters of the frictional treatment (indenter material, medium, load) of the 12Kh18N10T chromium-nickel austenitic steel have been optimized for the criteria of strain hardening and the quality of the surface being treated. The paper studies effect of the multiplicity of the frictional action of a synthetic diamond indenter at room temperature in an argon medium and the loading temperature ranging between -196 °C and +250 °C on the hardening, phase composition and fine structure of the surface layer of the steel. It has been found that the completeness of the strain-induced $\gamma \rightarrow \alpha'$ martensitic transformation in the surface layer of the steel is strongly dependent on the multiplicity and temperature of loading and that the level of hardening rises with the multiplicity of action, but shows little dependence on the temperature of frictional treatment.

INTRODUCTION

Nanostructuring frictional treatment with a sliding indenter is an effective method for increasing the strength and tribological properties of thermally non-hardenable austenitic chromium-nickel steels [1]. It is important in practical and scientific terms to optimize the conditions of frictional treatment not only for the criteria of effective hardening and ensuring a high-quality surface (low roughness, the absence of adhesive bonding centers or surface damage) [2], but also the formation of the required structural-phase state of the surface layer. For metastable austenitic steels, it is especially urgent, since hardening deformation processing is accompanied by the formation of strain-induced α' -martensite in a surface layer [1]. It is sometimes undesirable since it may result in poorer corrosion properties [3]. Therefore, it seems important to study if it is possible to control the phase composition on the surface of austenitic steel due to a change not only in the multiplicity of the deformation action, but also in the temperature of frictional treatment. As is known [4], low temperatures may intensify strain-induced transformation, whereas heating causes suppression of the $\gamma \rightarrow \alpha'$ -martensitic transformation in metastable Cr-Ni austenitic steel under friction.

The paper aims at studying the effect of the process conditions of frictional treatment (indenter material, medium, load, multiplicity and temperature of loading) on the quality of the final surface, the hardening and structural-phase transformations in the surface layer of austenitic steel.

EXPERIMENTAL PROCEDURE

The steel 12Kh18N10T (0.10 C, 17.72 Cr, 10.04 Ni, 0.63 Ti, 1.33 Mn, 0.57 Si, 0.227 Mo, 0.064 Co, 0.014 Nb, 0.057 Cu, 0.031 P, 0.014 S, the rest Fe, wt.%) was studied. Specimens sized 98×38×8.6 mm were subjected to water

quenching from 1050 °C, mechanical grinding and electrolytic polishing. In order to study the effect of the process parameters of frictional treatment, the loading was performed with a semi-spherical indenters of radii $R=2.5\text{--}3.0$ mm made of different materials, in different media, under loads P , the average speed of reciprocating motion $V=0.05$ m/s, stroke length $l=29$ mm, 0.1-mm indenter displacement after each double stroke and five indenter passages ($n=5$). The frictional treatment under optimized conditions was performed with an indenter made of synthetic diamond with $R=3$ mm, in a non-oxidizing argon medium under $P=392$ N and $n=1\text{--}11$, and at the loading temperature ranging between -196 °C and 250 °C with $n=1$ and $P=392$ N. The treatment at negative loading temperatures was performed in a liquid nitrogen medium. The surface roughness was examined on a Wyko NT-1100 optic profilometer, the microhardness was studied on a LEICA device under a load of 0.245 N, the phase composition was analyzed by a SHIMADZU XRD-7000 X-ray diffractometer in $\text{Cr } k_\alpha$ irradiation, and the fine structure was investigated on a JEOL JEM-2100 transmission electron microscope (TEM).

RESULTS AND DISCUSSION

It was found during the selection of the process parameters of frictional loading (see table 1) that the most effective hardening (up to $\text{HV}0.025=685$) of the steel surface is achieved by frictional treatment with a synthetic diamond indenter under load $P=490$ N in a non-oxidizing argon medium. The surface roughness R_a is 115 nm. Treatment with an indenter made of natural diamond offers low values $R_a=60$ nm, but the lowest level of hardening ($\text{HV}0.025=515$). When loading was performed with a VK8 hard alloy indenter under loads $P=294\text{--}490$ N and a fine-crystalline dense boron nitride indenter under loads $P=196\text{--}245$ N with a liquid lubricoolant under conditions of evolving adhesion bonding, surfaces with high values of roughness $R_a=225\text{--}380$ nm and microhardness ($\text{HV}0.025=610\text{--}660$) are formed. Treatment with a synthetic diamond indenter in an argon medium with $P=392$ N forms a high-quality surface without bonding ($R_a=75$ nm), and a higher level of hardness is achieved ($\text{HV}0.025=590$) than when $P=294$ N ($\text{HV}0.025=505$). Thus, in terms of the criteria of ensuring intensive strain hardening and low surface roughness, the most optimal process conditions of frictional treatment is treatment with a synthetic diamond indenter in a non-oxidizing argon medium under the load $P=392$ N.

TABLE 1. The effect of the indenter material, the lubricating-cooling medium and normal load on the indenter P on the microhardness $\text{HV}0.025$ and roughness R_a of specimens made of the steel 12Kh18N10T, with $n=5$ indenter passages

Indenter Material	Lubricoolant	P, N	HV0.025	Ra, nm
Natural diamond	liquid lubricoolant	490	515	60
Synthetic diamond	argon	490	685	115
Synthetic diamond	argon	392	590	75
Synthetic diamond	argon	294	505	95
Synthetic diamond	air	490	660	125
VK8 hard alloy	liquid lubricoolant	490	635	380*
VK8 hard alloy	liquid lubricoolant	294	610	225*
Boron nitride DBN	liquid lubricoolant	245	660	255*
Boron nitride DBN	liquid lubricoolant	196	650	245*
Boron nitride DBN	liquid lubricoolant	147	545	150

* There was adhesion bonding under frictional loading

The TEM investigation has established that the initial structure of quenched steel is austenite with the presence of separate undissociated dislocations in polyhedral grains and the presence of dislocation clusters on some boundaries (fig. 1a). X-ray phase analysis reveals 100 vol. % of the γ -phase (austenite) in the initial steel structure.

Severe plastic strain implemented under friction loading results in a highly dispersed structure in a thin (5 to 10 μm) surface layer of austenitic steel. Circular reflections of $(111)\gamma$ and $(200)\gamma$ austenite are clearly visible on the diffraction pattern shown in fig. 1c. The dark-field image in the $(111)\gamma$ reflection shows that the size of many separate crystallites of austenite does not exceed 100 nm (fig. 1d). The presence of the circular reflection from $(220)\alpha$ strain-induced martensite on the micro-electron diffraction pattern shown in fig. 1c testifies that, besides γ -phase nanocrystals, in the layer under study there are strain-induced α' -martensite nanocrystals. Thus, according to the data from transmission electron microscopy, in the thin surface of the 12Kh18N10T austenitic stainless steel there appear fragmented nanocrystalline (with crystallites smaller than 100 nm and high-angle boundaries) and submicrocrystalline (with crystallites larger than 100 nm) martensitic-austenitic structures.

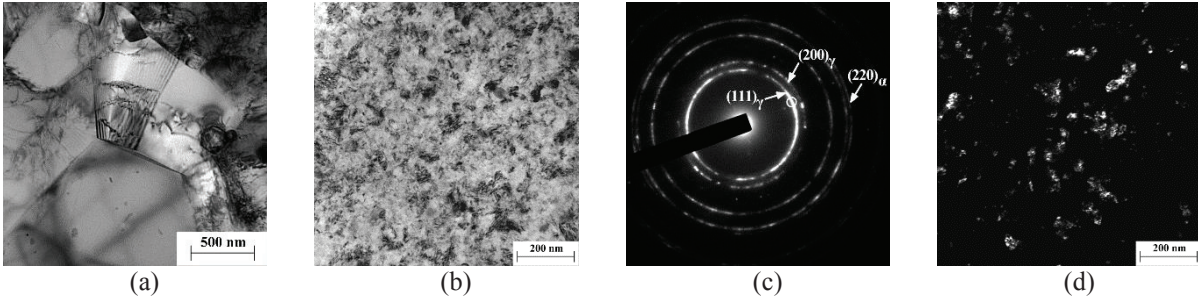


FIGURE 1. The structure of the surface layer of a 12Kh18N10T austenitic steel specimen in the as-quenched condition (a) and after frictional treatment with $n=11$ (b-d): (a-b) are bright-field images; (c) is diffraction; (d) is a dark-field image in the $(111)\gamma$ reflection

X-ray phase analysis and measurements of microhardness on the 12Kh18N10T steel surface demonstrate that the completeness of the strain-induced austenite transformation and the level of the hardening of the strained layer increase with the multiplicity of the frictional action of a synthetic diamond indenter (fig. 2a). As the number of indenter scans grows from $n=1$ to $n=11$, portion of strain-induced martensite on the surface of austenitic steel increases from 55 to 70 vol. % and the microhardness rises from $HV0.025=560$ to $HV0.025=710$ (the initial microhardness of quenched undeformed steel $HV0.025=220$). The total depth of the layer hardened by frictional treatment (when $n=11$) is $\sim 450 \mu\text{m}$ [1].

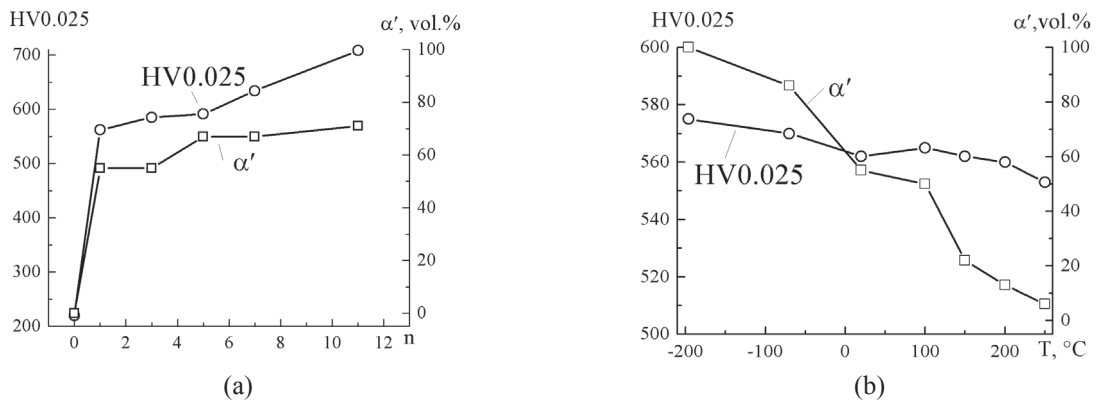


FIGURE 2. The effect of the number of indenter scans n (a) and the loading temperature when $n=1$ (b) on the quantity of strain-induced α' -martensite and microhardness $HV0.025$ on the surface of the 12Kh18N10T steel

X-ray phase analysis of the surface of the specimens subjected to frictional treatment at different temperatures has shown (fig. 2b) that the completeness of the strain-induced $\gamma \rightarrow \alpha'$ martensitic transformation in the surface layer of the austenitic 12Kh18N10T steel is strongly dependent on the temperature of frictional loading. Thus, at a loading temperature of -196°C , the quantity of α' -martensite in the surface layer reaches 100 vol. %. At the temperature of frictional treatment rises due to austenite stabilization to $\gamma \rightarrow \alpha'$ transformation, the quantity of strain-induced martensite on the loaded surface decreases continuously and, after frictional loading at $+250^\circ\text{C}$ it amounts to 5 vol. %. However, at all the temperatures of frictional loading, despite developing different phase compositions of the surface layer, close levels of strain hardening of the steel ($HV0.025=555-575$) are observed, fig. 2b. Consequently, heavily deformed austenite is close to strain-induced martensite in terms of hardness. This results from low carbon content in steel (0.10 wt. % C), which is insufficient for the effective hardening of the martensitic structure.

According to the data of transmission electron microscopy (fig. 3), in the thin surface layer of the 12Kh18N10T austenitic steel under frictional treatment (when $n=1$) there appear fragmented structures of strain-induced martensite (at the loading temperature of -196°C) and austenite (at the loading temperature of $+250^\circ\text{C}$). The dark-field images of the structure in martensitic $(110)\alpha$ and austenitic $(111)\gamma$ circular reflections shown in figs. 3b, d

testify that in the heavily disoriented fragmented structures of the thin surface layer of the 12Kh18N10T steel there are of both submicron-sized (150-200 nm) and nano-sized (below 100 nm) crystallites.

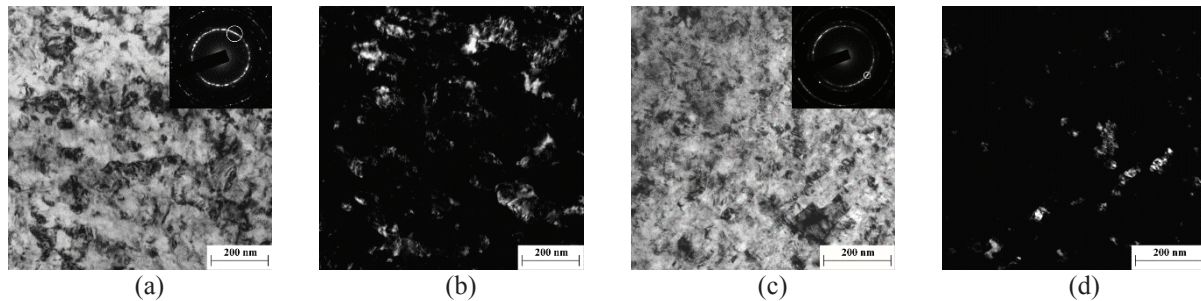


FIGURE 3. The structure of the surface layer of a 12Kh18N10T steel specimen after frictional treatment when $n=1$ at loading temperatures T of $-196\text{ }^{\circ}\text{C}$: (a, b) and $+250\text{ }^{\circ}\text{C}$ (c, d): (a), (c) are bright-field images; (b) is a dark-field image in the $(110)\alpha$ reflection; (d) is a dark-field image in the $(111)\gamma$ reflection

CONCLUSIONS

In the optimization of the process parameters of the frictional treatment of the metastable austenitic steel (grade 12Kh18N10T) in terms of ensuring intensive strain hardening and a high quality of the surface treated, advantages of using a synthetic diamond indenter and a non-oxidizing argon medium have been revealed. It has been demonstrated that the level of hardening and the completeness of strain-induced austenite transformation in the surface layer of the steel grows with the multiplicity of the frictional action. The completeness of the strain-induced $\gamma \rightarrow \alpha'$ martensitic transformation is also strongly dependent on the temperature of frictional loading; namely, as the temperature rises from $-196\text{ }^{\circ}\text{C}$ to $+250\text{ }^{\circ}\text{C}$, the quantity of strain-induced martensite decreases from 100 vol. % to 5 vol. %. However, when the temperature of frictional treatment varies in the range between $-196\text{ }^{\circ}\text{C}$ and $+250\text{ }^{\circ}\text{C}$, close levels of steel strain hardening can be reached. It has been found by transmission electron microscopy that, after frictional treatment, in the surface layer of the steel fragmented submicrocrystalline and nanocrystalline structures of strain-induced α' -martensite (at the loading temperature of $-196\text{ }^{\circ}\text{C}$) and austenite (at the loading temperature of $+250\text{ }^{\circ}\text{C}$) are formed, as well as two-phase martensitic-austenitic structures (at the loading temperature of $+20\text{ }^{\circ}\text{C}$).

ACKNOWLEDGMENTS

The work was done in the framework of the Complex Program of UB RAS (project No. 15-9-12-45) and the government assignment for IES UB RAS, theme No. 01201354598 supported by RFBR, project No. 15-08-07947.

REFERENCES

1. A. V. Makarov, P. A. Skorynina, A. L. Osintseva, A. S. Yurovskikh, R. A. Savrai, *Obrab. Metal. (Met. Work. Mat. Sci.)* **69** (4), 80–92 (2015).
2. V. P. Kuznetsov, A. V. Makarov, S. G. Psakhie, R. A. Savrai, I. Yu. Malygina, N. A. Davydova, *Phys. Mesomech.* **17** (4), 250–264 (2014).
3. T. Balusamy, T. S. N. Sankara Narayanan, K. Ravichandran, Il Song Park, Min Ho Lee, *Corr. Sci.* **74**, 332–344 (2013).
4. L.G. Korshunov, V.G. Pushin, N.L. Chernenko, V.V. Makarov, *Phys. Met. Metallogr.* **110** (1), 91–101 (2010).